

Robust Deep Network Learning of Nonlinear Regression Tasks by Parametric Leaky Exponential Linear Units (LELUs) and a Diffusion Metric

Enda D.V. Bigarella

^aIndependent Researcher, Starnberger Weg 7, Gilching, 82205, Germany

Abstract

This document proposes a parametric activation function (*ac.f.*) aimed at improving multidimensional nonlinear data regression. It is a established knowledge that nonlinear *ac.f.*'s are required for learning nonlinear datasets. This work shows that smoothness and gradient properties of the *ac.f.* further impact the performance of large neural networks in terms of overfitting and sensitivity to model parameters. Smooth but vanishing-gradient *ac.f.*'s such as ELU or SiLU have limited performance and non-smooth *ac.f.*'s such as RELU and Leaky-RELU further impart discontinuity in the trained model. Improved performance is demonstrated with a smooth “Leaky Exponential Linear Unit”, with non-zero gradient that can be trained. A novel diffusion-loss metric is also proposed to gauge the performance of the trained models in terms of overfitting.

Keywords: Deep Neural Network, Nonlinear Regression, Overfitting, Activation Function, Diffusion Loss

1. Introduction

It is typical in engineering applications that a modelled system is multidimensional, *i.e.*, a representative output parameter of the system depends on many system operational variables. The model might also be structured following a mesh-like combination of the system variables, which were input on a computational model or test bench for the data generation. In the example

Email address: enda.bigarella@gmail.com (Enda D.V. Bigarella)

to be addressed in this document, a metric of an electric motor efficiency is dependent on three variables, representative of the motor speed, power, and electric feed. This seemingly simple problem has proven to be surprisingly difficult to be trained for data regression. In an effort on Gaussian Process Regression (GPR) methods [1], the author developed a loss based on a diffusion operator to detect and avoid overfitting resulting from the highly nonlinear training landscape.

An argument in [2] stating that deep-learning methods naturally provides a Occam’s Razor behaviour has instigated the author to apply a neural network (NN) to the problem. There was an expectation that this property would naturally avoid overfitting as seen with the GPR models. The nature of the motor model has also raised some learnings in this deep learning context and are herein reported.

The scientific and engineering communities are interested in modelling techniques that are robust to parameters and that provide good generalisation. The selection of the activation function (*ac.f.*) of a NN heavily impacts such objectives, and it is known that nonlinear *ac.f.*’s are necessary to be able to model nonlinear datasets [3]. However, most of the literature focuses on large models for classification problems [4, 5, 6, 7], and regression problems are typically small [8] and the concern is usually with underfitting.

A dense feedforward NN was set up to learn the aforementioned motor model, for which relatively large depths and widths were required. In general, the “global” overfitting patterns of the GPR methods seen in [1] are not observed with the NN. As shown in Sect. 4.2, rather “localised” low-amplitude small-lengthscale features are observed – in this sense, “localised” refers to over-expression *between adjacent* data points, thus not a “global” long wavelength pattern spanning through many data points. In special, the regions where two of the variables are fast changing but the third one is not, seemed to exacerbate the issue.

A motivation to pursue a deeper understanding of the observed issues comes from this remark in [9], that “a priori knowledge of a particular task into a learning algorithm (...) generally improves performance, if the incorporated knowledge is relevant to the task.” The author proposes an *ad hoc* metric of the flexibility of the *ac.f.* as a ratio of its maximum and minimum gradients. In considering this metric, it can be observed that highly flexible *ac.f.*’s are prone to over-expressing in large models, whereas the conventional linear unit has zero flexibility and thus only represents linear functions (a common knowledge [3]). The current work proposes a paramet-

ric, trainable flexibility that enhances the a priori “fitness” of an *ac.f.* for more generalisable nonlinear learnings.

Furthermore, concern with *ac.f.* smoothness has motivated other work [5, 7], and the notion of trainable/adaptive coding in *ac.f.* has demonstrated successful behaviour [10, 11, 12]. This outcome is herein achieved with a simple *ac.f.* definition, termed Leaky Exponential Linear Unit (Leaky ELU, or LELU). Importantly, the focus here is broader in the sense that it focuses on a set of behavioural features of an *ac.f.* for generalisation, one of them being the discussed flexibility, but also robustness (*i.e.*, reduced dependency) with model size. Quoting [12] “there is no rule of thumb of choosing an optimal activation function.” Essentially, we want to decrease the effort in finding an optimal *ac.f.* by providing an adaptive framework that is able to code the degree of presence of particular phenomena in the input in a smooth and ever proportional way.

Another proposition in the current work is the use of a diffusion-like metric to gauge the performance of the NN, especially in terms of overfitting. As developed in [1], the “entropy-in-features” of the training data is computed via a modified Laplace operator and considered as a true label. Testing performed on a staggered mesh measures the entropy content of a trained model with respect to the true label, essentially meaning that a trained model should limit the amount of extra features it determines, and thus less “noise” stemming from overfitting.

The localised overfitting behaviour is demonstrated on canonical unidimensional problems, with model sizes representative of that for the motor model. It is shown that classical *ac.f.*’s have mixed performance in the problems whereas the proposed LELU is robust to model size. The observed properties of the LELU are further demonstrated in the motor model.

2. Activation Functions

The author herein proposes an *ad hoc* score of the “flexibility” (term inspired by [13]) of an *ac.f.* to serve as a proxy of its behaviour in data regression tasks. The flexibility score $\eta(\phi)$ is proportional to the ratio of the maximum and minimum slopes of an *ac.f.* ϕ , such that

$$\eta(\phi) = 1 - \frac{\min(\phi')}{\max(\phi')}. \quad (1)$$

This scores is zero for inflexible *ac.f.*’s, such as the Linear Unit (LU), which can only represent linear functions. On the other extreme, an *ac.f.* with

Table 1: Flexibility score of classical activation functions by application of Eq. 1. The parametrized activation functions affect the flexibility score by their control parameter.

Activation	$\eta(\phi)$
LU	0
tanh	1
ReLU	1
ELU [5]	1
Leaky ReLU [14, 4]	$1 - \alpha$
SiLU [15]	1.1
Softplus [9]	1
LELU	$1 - \beta$

score 1 is highly flexible. Table 1 shows the score for the *ac.f.*'s plotted in Fig. 1.

In the current work, it is shown that for *nonlinear regressions tasks* the following features of an *ac.f.*'s negatively impact the model performance:

- a higher flexibility score is more likely to present overfitting,
- discontinuous functions impart discontinuity into the trained data,
- vanishing gradient impairs training, irrespective if the function saturates at non-zero values [14],
- absence of negative values is too restrictive for neuron activation for smooth functions and limits their learning.

This motivates the proposal of a parametric *ac.f.* with a trainable parameter that overcomes these limitations and thus allows for faster and more robust training for nonlinear regression tasks. The family of activation functions, termed “Leaky Exponential Linear Unit” (Leaky ELU, or LELU), is given by

$$\text{LELU}(x, \beta) = \begin{cases} x & \text{if } x > 0 \\ \exp((1 - \beta)x) - 1 + \beta x & \text{if } x \leq 0 \end{cases} \quad (2)$$

where the trainable parameter β controls the slope of the activation function in the negative region (see Fig. 1).

The parametric LELU is constructed by imposing the following objectives for its features and behaviours

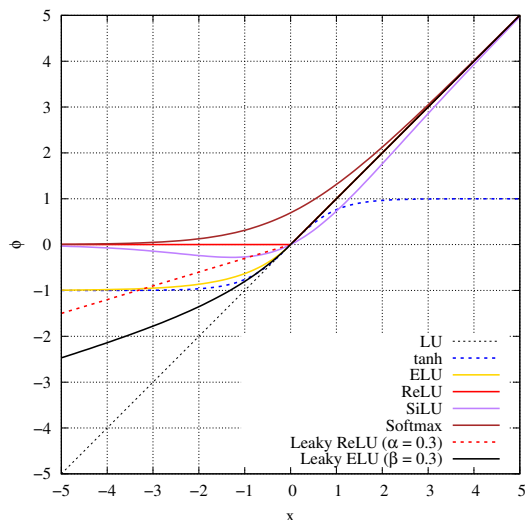


Figure 1: Graph of several activation functions.

1. monotonically continuous,
2. non saturating (non-null gradients),
3. to push the unit mean activation closer to zero.

These requirements are imposed onto the *ac.f.* construction to enhance the performance for nonlinear regressions tasks. The regression results show that this set of features inherently produces a behaviour similar to batch normalisation without the need for regularisation, as for instance explicitly required in [7, 16].

3. Model Description

The general aspects of the deep-learning model are initially presented. In the sequence, the diffusion-loss metric formulation is described.

3.1. Neural Network Configuration

A fully-connected feedforward NN is set up with n hidden layers each containing m neurons, and a linear-uniform single-neuron output, as sketched in Fig. 2. The NN is implemented in Python using the Keras library [17] and trained to minimise the mean absolute error (MAE) employing the Adam optimizer [18]. The minimisation of the MAE has provided better results for the regression tasks when compared to a mean squared error (MSE).

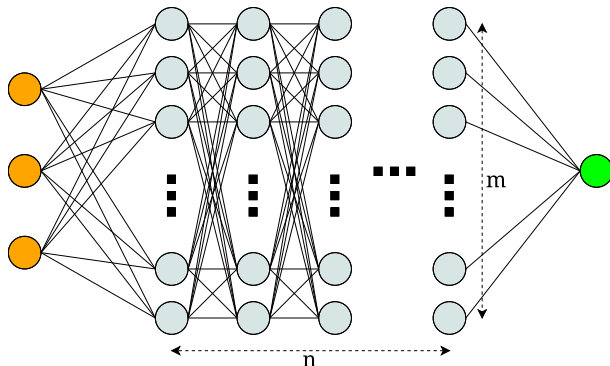


Figure 2: A vanilla feedforward neural network of depth n and width m , with three inputs and one output. The output layer is linear.

The learning rate is step-annealed based on the MAE loss – more details are later provided for each model. Neurons are initialised with a HeNormal distribution [4].

Regularization in regression tasks is essentially a trade-off: it helps prevent overfitting and can improve training stability, but by definition the minimum achievable training error is limited by the strength of the regularization. Therefore, no regularisation is used as default in the current work, nonetheless this aspect is also herein briefly assessed since it is a common practice.

The use of a custom diffusion operator as a *testing metric* of performance allows for training on the full dataset. This metric is assessed via its MSE and described in the following subsection.

3.2. Diffusion-Loss Metric

The diffusion-loss formulation herein applied follows the more complete description in [1]. This methodology allows for the creation of a hierarchical testing metric from the training data field without requiring splitting a training dataset into testing sets. Training is performed on the complete available dataset and offers best chance for generalisation.

The method for identifying oscillations uses a measure of the diffusion of the training data represented by a modified Laplace operator ∇ . This sensor in a $1d$ finite-difference context is computed as follows

$$\nabla y_i = \frac{1}{\Delta^2} \frac{|y_{i+1} - 2y_i + y_{i-1}|}{y_{i+1} + 2y_i + y_{i-1}}, \quad (3)$$

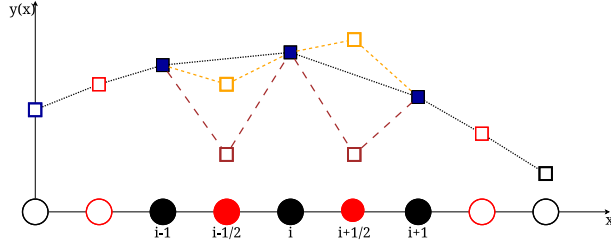


Figure 3: A one-dimensional mesh: the function values are shown by squares and the mesh nodes by circles. The original training mesh is shown as black nodes and the created staggered nodes, in red with half indices. Brown and orange squares show possible oscillations around node i .

for the i -th point of the mesh in Fig. 3, with Δ representing the mesh spacing, and y a positive property. In the currently proposed method, this diffusion sensor applied to the *training* data serves as the *true label*.

In order to create a suitable *testing metric* sensitive to overfitting in between training points, *staggered* nodes centred between the training points are created (shown in red in Fig. 3). An updated diffusion sensor $\tilde{\nabla}$ applied to these staggered nodes, indexed by half indices, is proposed

$$\tilde{\nabla}y_i = \frac{1}{3 (\Delta/2)^2} \frac{|\hat{y}_{i+1} - \hat{y}_{i+\frac{1}{2}} - \hat{y}_{i-\frac{1}{2}} + \hat{y}_{i-1}|}{\hat{y}_{i+1} + \hat{y}_{i+\frac{1}{2}} + \hat{y}_{i-\frac{1}{2}} + \hat{y}_{i-1}}, \quad (4)$$

with \hat{y} representing *predicted* function values, $\hat{y}_i = f(x)_i$, with $\hat{y} = y$ expected at the training points. This stencil is able to identify the “ringing/wiggling” features around the central node i . Therefore, deviations between a testing sensor (Eq. 4) and the true score (Eq. 3) can thus be used as testing metric in model training.

The creation of a staggered mesh in one dimension as shown in Fig. 3 is straightforward since a central node only has a single neighbour to either its side. On a multidimensional case, an approach based on a single staggered mesh built on centroids of the original mesh cells is proposed. In this approach, we are required to use the centre-crossing diagonals (composed of pairs of antipodal points) as an *ad-hoc* means to compute Laplace operators. The resulting staggered mesh for a $3d$ case is shown in Fig. 4.

The *staggered* Laplace-operator diffusion sensor written for a centre-crossing

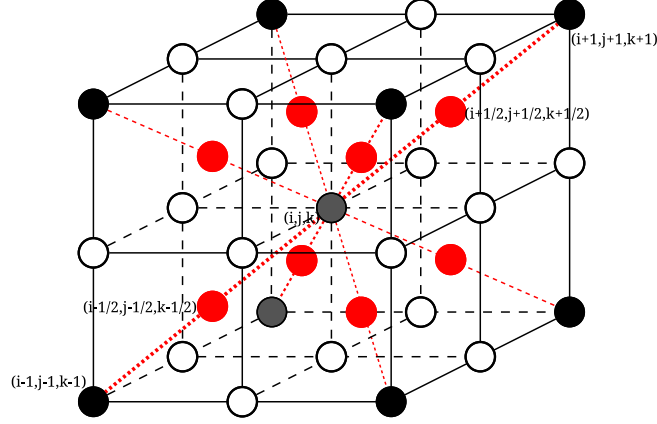


Figure 4: The original multidimensional training mesh shown as black points and the created cell-centred staggered points shown in red, with half indices. The diffusion sensors are computed along the centre-crossing diagonals shown in red. Filled symbols are used for the sensor computations for the central node $((i, j, k)$ in $3d$, for instance).

diagonal p of the node (i, j, k) in Fig. 4 is given by

$$\tilde{\nabla} y_{i,j,k}^p = \frac{1}{3 (\Delta/2)^2} \frac{|y_{i+1,j+1,k+1} - y_{i+\frac{1}{2},j+\frac{1}{2},k+\frac{1}{2}} - y_{i-\frac{1}{2},j-\frac{1}{2},k-\frac{1}{2}} + y_{i-1,j-1,k-1}|}{y_{i+1,j+1,k+1} + y_{i+\frac{1}{2},j+\frac{1}{2},k+\frac{1}{2}} + y_{i-\frac{1}{2},j-\frac{1}{2},k-\frac{1}{2}} + y_{i-1,j-1,k-1}}, \quad (5)$$

and for the true label

$$\nabla y_{i,j,k}^p = \frac{1}{\Delta^2} \frac{|y_{i+1,j+1,k+1} - 2y_{i,j,k} + y_{i-1,j-1,k-1}|}{y_{i+1,j+1,k+1} + 2y_{i,j,k} + y_{i-1,j-1,k-1}}. \quad (6)$$

The complete $3d$ diffusion sensors for the node (i, j, k) are given by the summation over all centre-crossing diagonals resulting in

$$\nabla y_{i,j,k} = \sum_{p=1}^4 \nabla y_{i,j,k}^p, \quad \tilde{\nabla} y_{i,j,k} = \sum_{p=1}^4 \tilde{\nabla} y_{i,j,k}^p. \quad (7)$$

Note that the diffusion sensors are only computed at the interior of the original mesh, where the complete stencil is available. The reader is referred to [1] for further and more general discussions and information about the methodology as well as snippets of code implementation.

4. Results and Discussions

We are interested in multidimensional problems that typically require large models to capture all their features. The author argues that using

canonical problems with isolated features and fitting small NNs to them do not guarantee generalisation of the approach for those large, real-world problems. We want to be able code the degree of presence of series of particular phenomena that might compose large problems. Therefore, in this work, we take large NNs that are required to represent large, complex models, and apply them to canonical problems in search of *ac.f.*'s that offer robustness whilst coding the degree of presence of different and composed phenomena. The goal is to provide an *ac.f.* that works well regardless of model size and that can scale effectively from small to large networks, thereby enabling potentially more robust and less time consuming regression tasks.

4.1. Unidimensional Problems

The proposed unidimensional problems¹ represent certain important features of the target motor model. A hyperbolic tangent function is chosen for its non-monotonic change of slope, whereas an exponential function is chosen for its fast change of properties. Numerical experiments with a NN of depths $n = [7, 8]$ and widths $m = [120, 240]$ (fixed per layer) are executed for the *ac.f.*'s listed in Table 2.

4.1.1. Hyperbolic Tangent Function

A $1d$ equation given by $f(x) = 0.5 + 0.5 \tanh(5x)$, $x \in [-1, 1]$ is used to generate two sets of equally spaced, noiseless (7, 14) training points. The model is trained for 15000 epochs with batch size 3. The learning rate is scheduled in the range $[1e - 3, 1e - 6]$ with factor 0.5, patience 500, and cooldown 100.

Table 2 presents the training losses and diffusion metrics of the trained model. The MAEs are generally low and care must be taken that the models are not tending to memorise the training points, the performance of the models is therefore truly assessed by the diffusion metric. The SiLU and LELU ($\beta = 0.3$) achieve low MAE and low diffusion losses, and the performance is not strongly lost with the reduction of the number of training points. This result is indicative of less overfitting, which is corroborated by the function plots in Fig. 5. Strongly overfitting is observed with some *ac.f.*'s in this setup, whereas the proposed LELU is relatively robust to the change in the number of training points. Not shown for the sake of conciseness, very similar results are observed with a 7×120 model as well.

¹Source files available in http://github.com/ebiga/nm_1d_overfit_ex

Table 2: Losses of the trained models for the hyperbolic tangent data.

Activation	Training MAE $\times 10^{-6}$		Diffusion MSE $\times 10^{-3}$	
	14pts	7pts	14pts	7pts
Leaky ReLU ($\alpha = 0.2$)	14	10	90	216
LELU ($\beta = 0.3$)	20	27	16	25
LELU ($\beta = 0.4$)	22	101	49	72
LELU ($\beta = 0.6$)	54	68	15	73
Softplus	71	21	16	220
SiLU	23	19	13	49
tanh	17	8	156	372
ELU	17	88	55	234
ReLU	8	5	125	241

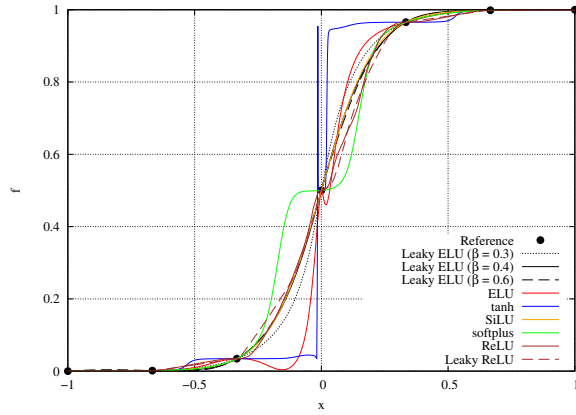
4.1.2. Exponential Function

A 1d exponential equation given by $f(x) = 0.1^x$, $x \in [-1, 1]$ is used to generate a set of 12 equally spaced, noiseless training data points. The model is trained for 20000 epochs with batch size 3. The learning rate is scheduled in the range $[1e - 3, 2e - 7]$ with factor 0.5, patience 500, and cooldown 100.

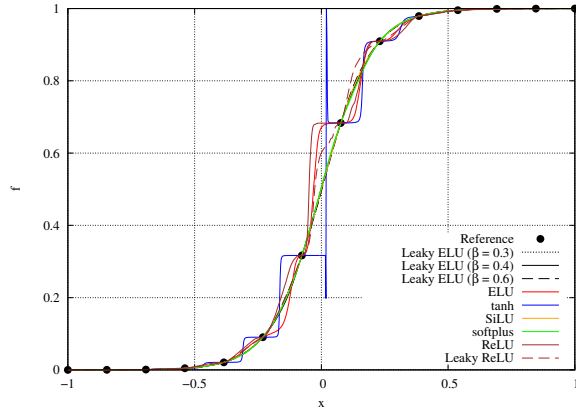
Table 3: Losses of the trained models for the exponential function data.

Activation	Training MAE $\times 10^{-6}$		Diffusion MSE $\times 10^{-3}$	
	$n = 8$	$n = 7$	$n = 8$	$n = 7$
Leaky ReLU ($\alpha = 0.2$)	4	31	12	16
LELU ($\beta = 0.3$)	50	19	3	2
LELU ($\beta = 0.4$)	24	33	2	2
LELU ($\beta = 0.6$)	34	62	1	1
Softplus	120	133	5	2
SiLU	7	25	13	14
tanh	21	14	28	37
ELU	18	12	18	20
ReLU	4	5	25	19

Table 3 presents the training losses and diffusion metrics of the trained model. As in the previous case, the lower the MAE, the higher is the tendency



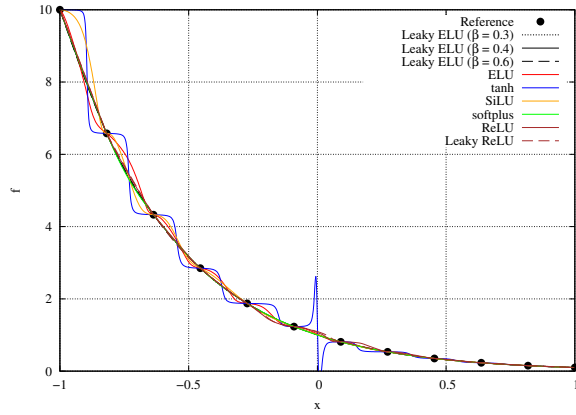
(a) 7 training points.



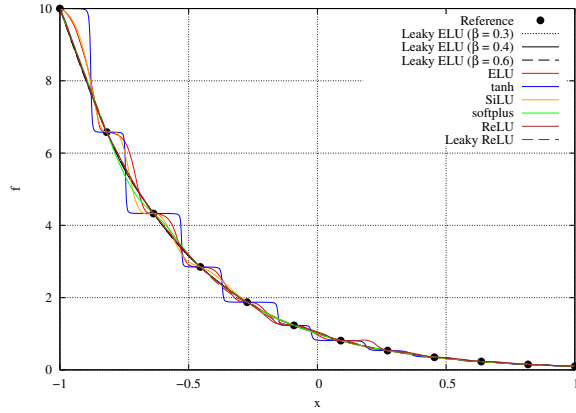
(b) 14 training points.

Figure 5: Trained hyperbolic tangent function plots for the different activation functions.

of the model to memorise the training data, with a resulting increase in the diffusion metric. For this case, both SiLU and Softplus show a poorer performance and trade the training and diffusion (overfitting) errors. The LELUs are able to adequately meet both low MAE and diffusion errors. The trained model predictions are plotted in Fig. 6. As in the previous case, different levels of overfitting are observed with the classical *ac.f.*'s in this setup, whereas generally robust results are obtained with the LELU.



(a) Depth 7.



(b) Depth 8.

Figure 6: Trained exponential function plots for the different activation functions.

4.1.3. Exponential Function and a Single Neuron

The previous problem is reduced to a set of three training points, $x_i = (-1, 0, 1)$, which a single neuron shall learn. This exercise can be performed by hand and two of the three points can be exactly matched. The obtained neuron parameters are used to infer a function as shown in Fig. 7, plotted along the *ac.f.* derivatives and training errors.

In terms of training error (at the third point), ReLU, SiLU and Softplus produce smaller errors whereas the LELU has the largest. However, ReLU, ELU, SiLU and Softplus tend to null gradients whereas the Leaky ReLU and LELU produce a strong signal that indicates that that behaviour cannot be

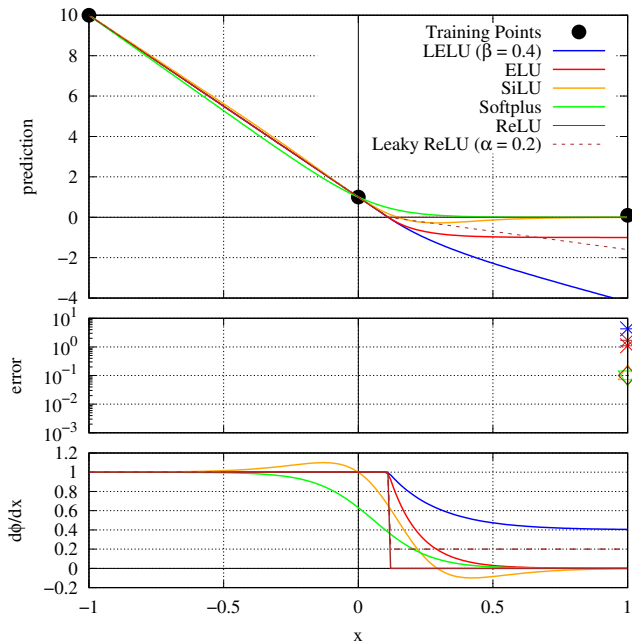


Figure 7: Predictions with a single neuron trained for the three data points.

coded – the task therefore requires and should be taken by the next of kin on a larger model.

From the perspective of learning nonlinear regression tasks, such weak signal is less than ideal. The gradient and Hessian of the loss can be computed by hand for this simple problem. This operation shows that the weak *ac.f.*'s produce a vanishing loss gradient and higher conditioned Hessians, which is indicative of the tendency to poor learning and overfitting. The LELU on the other hand produces a clear gradient and a lower conditioned Hessian. With this simple exercise, the author intends to anecdotally show that the higher “flexibility” of the *ac.f.* is incurring in a weak signal for subsequent neurons and is a potential cause of instability showing as overfitting.

4.1.4. Other Findings with the Unidimensional problems

It is interesting to note that some *ac.f.*'s struggle around $x = 0$ in both case studies, even when this point is *not* a training data. A thorough explanation is challenging for a large model [16], but the author believes this can be partially understood by a similar analysis of the gradient as in the

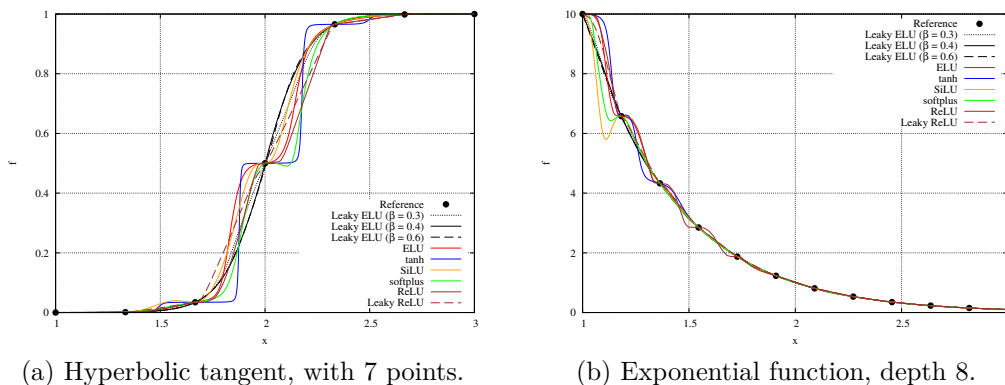


Figure 8: Trained function plots for the different activation functions on a positive range of x .

previous subsection. The loss-gradient is proportional to the summation of the gradient of the *ac.f.* times the training point coordinate. If the training point coordinate tends to zero, or adjacent training points cross $x = 0$, this can further induce the loss gradient summation to vanish or “flicker”, and to destabilize the learning on an already unstable model setup. This behaviour is confirmed with a simple shift in x by two units, as shown in Fig. 8, in which the local instability around $x = 0$ is removed for the unstable models. Note that SiLU actually lost performance and presents overfitting, opposed to the behaviour shown in Fig. 5a, which corroborates the borderline stability of the model.

Another observation is that discontinuous *ac.f.*’s generate discontinuous trained models in both exercises. In these and some other setups not shown in here, the discontinuous *ac.f.*’s rather often default to piecewise linear connection between the training points. Even when this was not the case, the trained model is still discontinuous, as seen in Figs. 5, 6 and 8.

The adopted canonical problems indicate that classical *ac.f.*’s lack robustness with the problem setup for nonlinear regressions tasks when trained by large models. The proposition of the objectives in Sect. 2 for the LELU construction aims at mitigating the reported issues.

4.1.5. Other Approaches to Decrease Overfitting

By assuming that the author has been successful in the beginning of this section to justify the most obvious criticism against these exercises, *i.e.*, the

adopted model sizes, other strategies also merit further discussions. Known strategies to deal with overfitting, namely, regularisation and smaller learning rates for longer epochs were also evaluated. The results are not shown for the sake of conciseness since the outcomes are as expected, *i.e.*, a decrease in the overfitting is achieved however at the expense of considerably higher training MAEs and/or computational resources. Both L1 and L2 regularisations, with constant strength $1e - 4$, are able to reduce or remove (L1 regularisation) overfitting, however at the expense of 10x or larger training MAEs. In terms of learning rates, an example with the ELU required reduction of half of the initial learning rate, and 10x longer training epochs.

The LELU is able to achieve adequate results without those penalties. It can robustly learn the nonlinear regression task without memorising the training data. This behaviour is further confirmed on the more complex model discussed in what follows.

4.2. Electric Motor Model

The noise-free system model described in the introduction is composed of a 3d mesh of $(param1, param2, param3) = (19 \times 15 \times 5)$ points, shown in Fig. 9. The problem shows a fast change of behaviour along *param1* and an even faster one with *param2*, which combine at one corner of the operational envelope of the motor. The behaviour with *param3* shows as the “thickness” of the wireframe, and it changes with both other parameters and collapses at their lower borders. A nonlinear feature can also be observed approaching the maximum limits of the *param1* range.

The dataset is normalised so as to keep unitary mesh spacing in all dimensions to avoid cell skewness (which also favours the computation of the diffusion differentials), and kept in the positive range to support the more sensitive *ac.f.*’s. For the current study the trained data must exactly reproduce the noise-free training information [1]. A noiseless training is generally more challenging and is an additional reason for this choice in the current exercise.

A numerical experiment with the implemented² NN with combinations of depth $n = [6, 7, 8]$ and width $m = [80, 120, 240, 360]$ (fixed per layer) is executed. The model is trained for 9000 epochs with batch size 35. The learning rate is scheduled in the range $[1e - 3, 1e - 5]$ ($5e - 4$ for the models

²Source files available in http://github.com/ebiga/gpr_aniso_trials

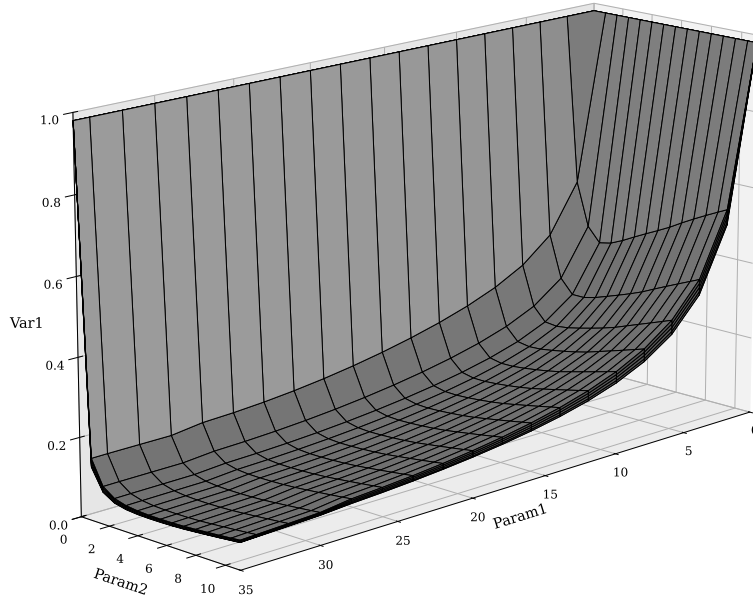


Figure 9: Wireframe view of the motor model mesh with the third dimension shown as the “thickness” of the wireframe. The third dimension collapses at the lower borders.

with width 360 and the 8×240 case) with factor 0.5, patience 250, and cooldown 50.

Figure 10 shows the MAE and diffusion metrics for the different model sizes (indexed by $m^n/1e12$ in the plots). The tendency to overfit shows as a lack of “convergence” of the MAE with the increase in the model size. For this complex problem the mean errors do not show large differences between the “good” and “bad,” so visual inspection is also necessary. Nonetheless, it can be seen that both metrics are lower with the LELU and are also more robust to model size. SiLU and Softplus do not present any favourable behaviour as partially seen with the canonical problems. The conclusions above are corroborated by the slice plots in Figs. 11 and 12.

Figure 11 shows slices along *param2*, which is the fast-changing variable. The tanh and ReLU results are not shown due to the poor performance. The region *param2* = [0, 2], where the highest slopes are seen, presents a tough task for the *ac.f.*’s. Considerable “localised” overfitting is observed for the ELU, SiLU and Softplus. Interestingly, the less flexible *leaky ac.f.*’s show lower overfitting content and also less dependency on the model size. This

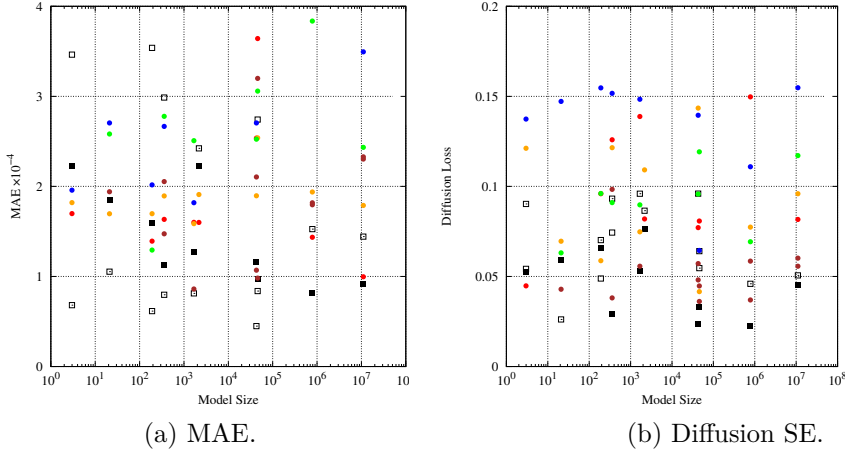


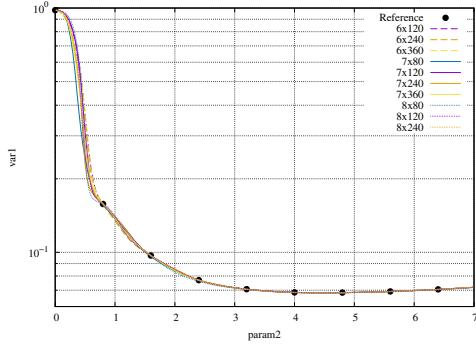
Figure 10: Trained model losses for the electric motor.

nice behaviour prompted the current effort into assembling this property into a new *ac.f.* The Leaky ReLU results are “kinky” though and such behaviour is not ideal. The proposed LELU with $\beta = 0.4$ shows a robust performance, indicating that the lower flexibility and smoothness are indeed advantageous.

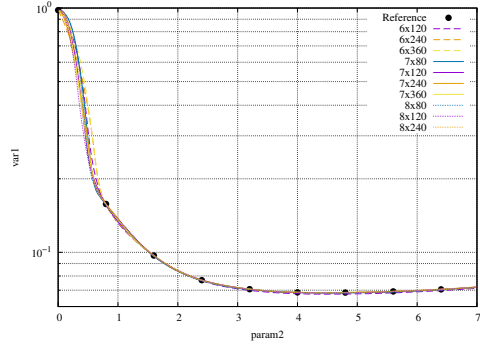
Figure 12 shows similar slices along the tight- and slow-changing *param3*. This slice allows for interesting behaviours to be more closely assessed, *i.e.*, the *spread* of the *ac.f.* with different model sizes and the *capacity to code* small values. The less flexible *leaky ac.f.*’s clearly show tighter and more representative capacity. SiLU and Softplus are also able to demonstrate a tighter spread, albeit with an offset error to the training data, whereas ELU is generally poorly behaved.

By inspection of *ac.f.* graphs in Fig. 1, it can be seen that both SiLU and Softplus present a wider range of slowly changing gradient, or in other words, ELU has a sharper gradient change. In the SiLU case, the gradient is actually never zero in the range plotted in Fig. 1. This observation has further prompted the effort into coding this property into the LELU. As seen in Fig. 1, this *ac.f.* slowly changes slopes and is therefore smoother than other *ac.f.*’s, thereby enabling a stronger a priori fitness for generalisable nonlinear regressions.

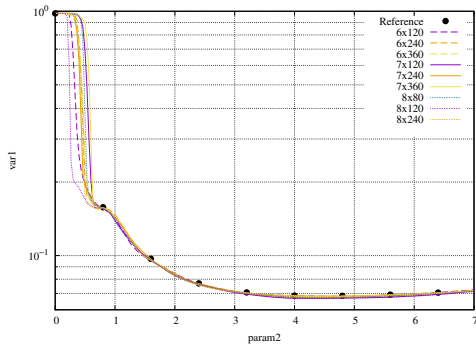
For this motor model the LELU with $\beta = 0.4$ provides the most agreeable results. Upon careful visual inspection of each NN result (see Fig. 13), depth 6 is not enough to capture all features, whereas depth 7 is able to do so



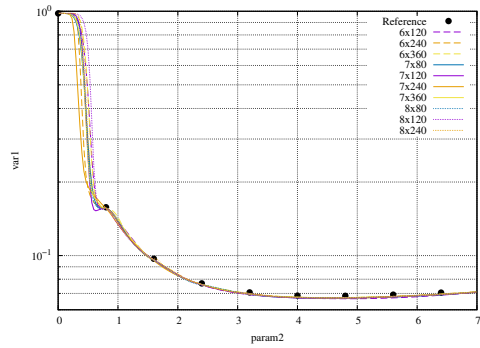
(a) LELU ($\beta = 0.2$)



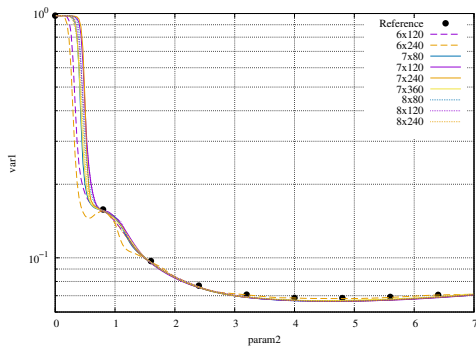
(b) LELU ($\beta = 0.4$)



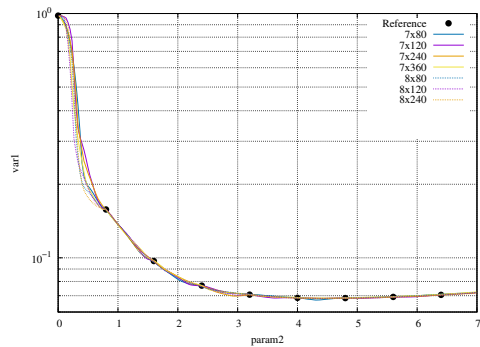
(c) ELU



(d) SiLU



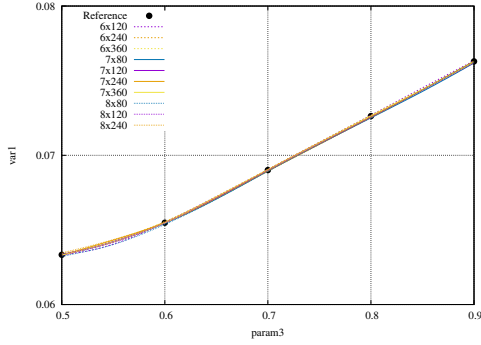
(e) Softplus



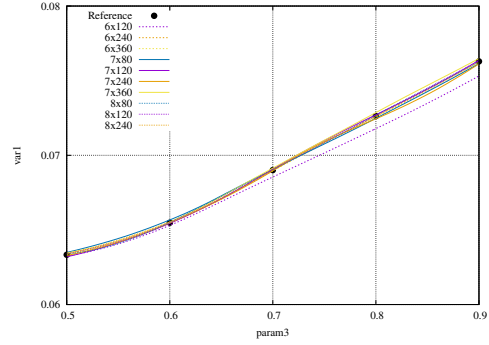
(f) Leaky ReLU ($\alpha = 0.2$)

Figure 11: Trained electric motor model predictions sliced at $(param1, param3) = (28, 0.8)$ for different activation functions and model sizes.

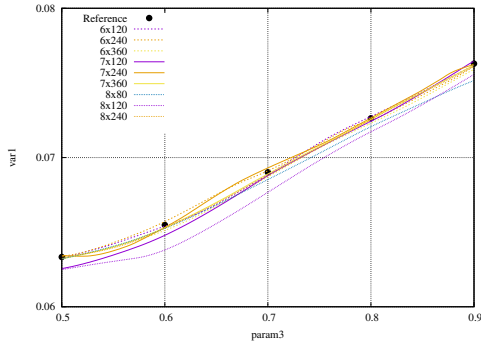
but the MAE still indicates some distance (error) to the training points.



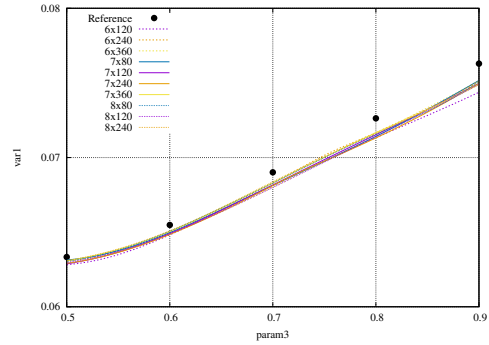
(a) LELU ($\beta = 0.2$)



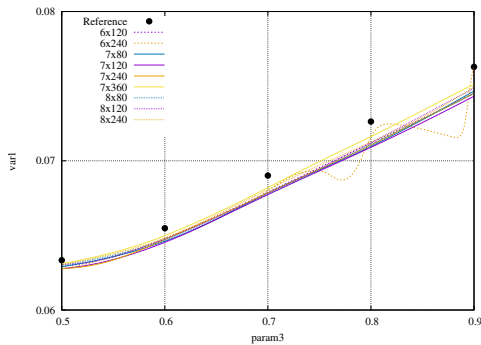
(b) LELU ($\beta = 0.4$)



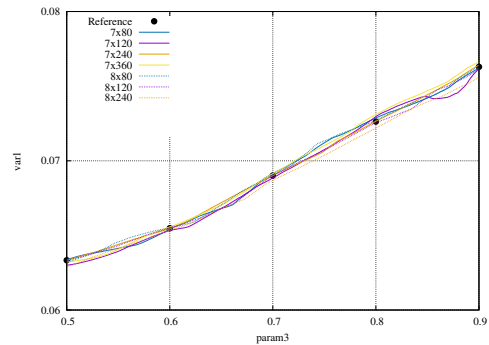
(c) ELU



(d) SiLU



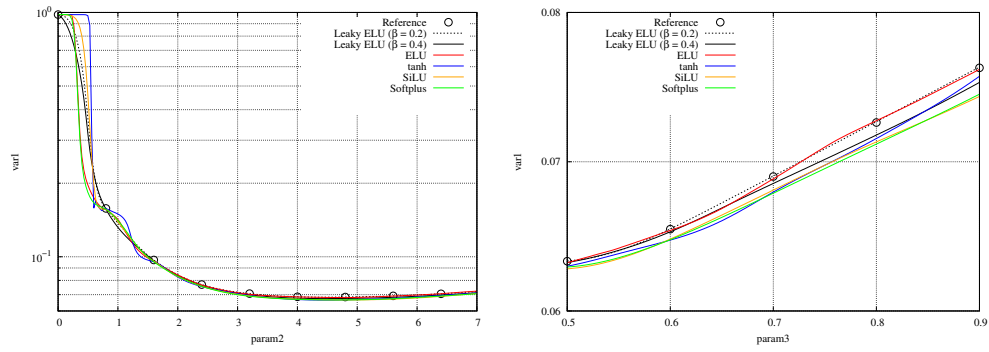
(e) Softplus



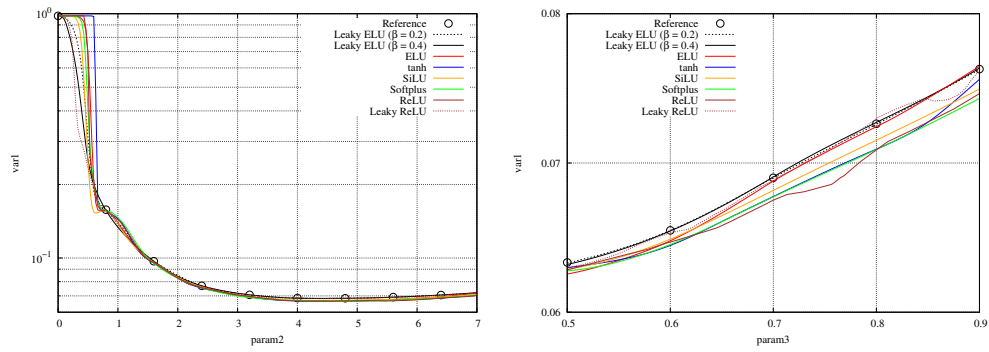
(f) Leaky ReLU ($\alpha = 0.2$)

Figure 12: Trained electric motor model predictions sliced at $(param1, param2) = (28, 7.2)$ for different activation functions and model sizes.

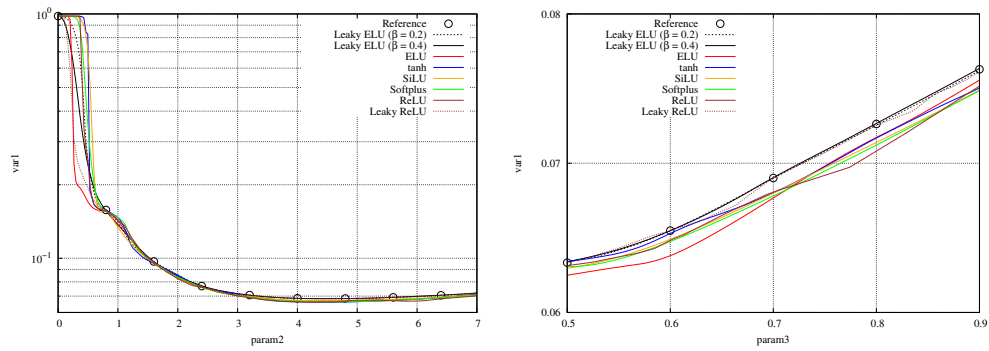
Generally at least width 120 is necessary for acceptable results.



(a) 6×120



(b) 7×120



(c) 8×120

Figure 13: Model size effect on the electric motor predictions for different activation functions.

It is worth revisiting the discussion in Sect. 4.1.5. Except from reducing the model size, which is in fact hopefully clear now the need for such larger

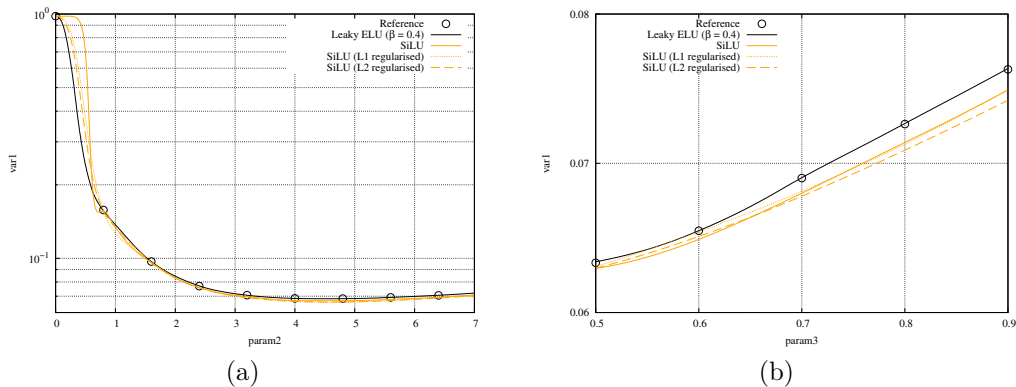


Figure 14: Regularisation effect on the electric motor predictions for the 8×120 model.

models, the other techniques to control overfitting also apply to the motor model. As shown in Fig. 14, both L1 and L2 regularisations (strength $1e-4$) reduce the overfitting behaviour of the SiLU, at the expense of representation of training points. The MAE increase by more than a factor of 6 in these cases and the performance does not improve over the LELU ($\beta = 0.4$). Another strategy is to implement a change of variables, for instance a power correction $\tilde{y} = y^{0.1}$, to reduce the large differences in the max and min values. A model trained on this function learns faster and easier, however the resulting errors when brought back to the original scale are also very large, which defeats the purpose. As already observed with the canonical problems, the LELU seems to provide adequate results without those drawbacks and extra steps.

5. Concluding Remarks

A parametric activation function for nonlinear regressions tasks that is monotonically smooth, with a non-null gradient at the negative region, is developed. The proposed *ac.f.* is termed Leaky Exponential Linear Unit (or Leaky ELU, or LELU). The non-null gradient is proposed as a means to control an *ad hoc* score of the flexibility of an *ac.f.* and is a trainable parameter. Available nonlinear *ac.f.*'s have generally high flexibility scores which seem to be associated with proneness to overfitting. A null flexibility score can only represent linear data, on the other hand.

Smoothness is sought to avoid coding discontinuities at the predictions of the trained model. This is shown to be a result of the ReLU and Leaky ReLU

ac.f.'s. The Leaky ReLU however has a trainable flexibility and this is shown to support the claim of beneficial and robust behaviour of this property for nonlinear regression tasks.

The results with the LELU are promising for highly nonlinear regressions tasks and large models. Its properties implicitly produce a behaviour similar to regularisation without strong penalisation of the training errors. The LELU does not show evidence of trading off training error with the overfitting/testing metric, at least not as strongly as other *ac.f.*'s. It also shows less sensitivity with model size and training points for nonlinear regression tasks.

Another proposition in the current work is a metric to identify overfitting. The method is based on a modified Laplace operator and tests for oscillation in the interior of the training mesh cells. A true label is provided by the modified Laplace operator applied to the original training nodes, which acts as a measure of the “entropy-in-features” contained in the training data. A *trained* model must limit (ideally avoid) the amount of extra features it determines based on its diffusion metric. The testing points must be created on a staggered fashion to be able to gauge any excess entropy in the interior of the mesh cells. With the proposed method, the model can be trained on all available training points.

The author expects the proposed methods to be generalisable to other machine learning or dataset strategies. The observed properties of the proposed LELU should reduce the workload to select a good model setup and is as a such a highly desirable behaviour. The Laplace operator with its measure of the diffusion of a system provides a powerful tool for detection (and prevention) of overfitting in data regression. They should provide a sure hand in the process of implementing a model by bringing more robustness and clearer metrics.

References

- [1] E. D. V. Bigarella, Prevention of overfitting on mesh-structured data regressions with a modified Laplace operator (2025). doi:<http://dx.doi.org/10.2139/ssrn.5280384>.
- [2] C. Mingard, H. Rees, G. Valle-Pérez, A. A. Louis, Deep neural networks have an inbuilt Occam’s razor, JNat Commun 16 (220) (2025). doi:<https://doi.org/10.1038/s41467-024-54813-x>.

- [3] I. Goodfellow, Y. Bengio, A. Courville, Deep Learning, MIT Press, 2016, <http://www.deeplearningbook.org>.
- [4] K. He, X. Zhang, S. Ren, J. Sun, Delving deep into rectifiers: Surpassing human-level performance on ImageNet classification (2015). arXiv:1502.01852.
URL <https://arxiv.org/abs/1502.01852>
- [5] D.-A. Clevert, T. Unterthiner, S. Hochreiter, Fast and accurate deep network learning by Exponential Linear Units (ELUs) (2016). arXiv:1511.07289.
- [6] P. Ramachandran, B. Zoph, Q. V. Le, Searching for activation functions (2017). arXiv:1710.05941.
URL <https://arxiv.org/abs/1710.05941>
- [7] N. Boullé, Y. Nakatsukasa, A. Townsend, Rational neural networks (2020). arXiv:2004.01902.
URL <https://arxiv.org/abs/2004.01902>
- [8] A. D. Jagtap, G. E. Karniadakis, How important are activation functions in regression and classification? A survey, performance comparison, and future directions (2022). arXiv:2209.02681.
URL <https://arxiv.org/abs/2209.02681>
- [9] C. Dugas, Y. Bengio, F. Bélisle, C. Nadeau, R. Garcia, Incorporating second-order functional knowledge for better option pricing, in: T. Leen, T. Dietterich, V. Tresp (Eds.), Advances in Neural Information Processing Systems, Vol. 13, MIT Press, 2000.
URL https://proceedings.neurips.cc/paper_files/paper/2000/file/44968aece94f667e4095002d140b5896-Paper.pdf
- [10] L. Hou, D. Samaras, T. M. Kurc, Y. Gao, J. H. Saltz, Neural networks with smooth adaptive activation functions for regression (2016). arXiv:1608.06557.
URL <https://arxiv.org/abs/1608.06557>
- [11] A. D. Jagtap, K. Kawaguchi, G. Em Karniadakis, Locally adaptive activation functions with slope recovery for deep and physics-informed

- neural networks, *Proceedings of the Royal Society A: Mathematical, Physical and Engineering Sciences* 476 (2239) (2020) 20200334. doi:10.1098/rspa.2020.0334.
- [12] A. D. Jagtap, Y. Shin, K. Kawaguchi, G. E. Karniadakis, Deep Kronecker neural networks: A general framework for neural networks with adaptive activation functions, *Neurocomputing* 468 (2022) 165–180. doi:<https://doi.org/10.1016/j.neucom.2021.10.036>.
- [13] D. M. Hawkins, The problem of overfitting, *Journal of Chemical Information and Computer Sciences* 44 (1) (2004) 1–12. doi:10.1021/ci0342472.
- [14] A. Maas, A. Hannun, A. Ng, Rectifier nonlinearities improve neural network acoustic models, in: *Proceedings of the International Conference on Machine Learning*, Atlanta, Georgia, 2013.
- [15] D. Hendrycks, K. Gimpel, Gaussian error linear units (GELUs) (2023). arXiv:1606.08415.
URL <https://arxiv.org/abs/1606.08415>
- [16] X. Hu, W. Liu, J. Bian, J. Pei, Measuring model complexity of neural networks with curve activation functions (2020). arXiv:2006.08962.
URL <https://arxiv.org/abs/2006.08962>
- [17] F. Chollet, et al., Keras, <https://keras.io> (2015).
- [18] D. P. Kingma, J. Ba, Adam: A method for stochastic optimization (2017). arXiv:1412.6980.
URL <https://arxiv.org/abs/1412.6980>